Velocity Dependence of the Differential Cross Sections for the Scattering of Atomic Beams of K and Cs by Hg†

FRED A. MORSE* AND RICHARD B. BERNSTEIN
Chemistry Department, University of Michigan, Ann Arbor

(Received July 16, 1962)

Measurements of the velocity dependence of the angular intensity distribution of potassium and cesium beams scattered by a crossed beam of mercury are presented. The alkali beam was velocity selected, with a triangular velocity distribution (half-intensity width 4.7% of peak velocity); the velocity was varied over the range 185–1000 m/sec. The Hg beam had a thermal distribution; the average Hg speed was ~235 meters per second. The scattering data have been converted to the center-of-mass system. The angular distributions show the expected strong forward scattering and evidence the phenomenon of rainbow scattering. The energy dependence of the rainbow angle is used to evaluate the interatomic potential well depth, interpreted as the dissociation energy D_e of the $^2\Sigma^+$ molecular ground state. Values (in erg$\times 10^{14}$) thus obtained ($\pm 5\%$) are 7.4_6 for KHg and 7.7_2 for CsHg. Absolute values of differential cross sections could not be obtained; only relative cross sections $D(\theta)$ are reported. The observed low-angle behavior $D(\theta) \propto \theta^{-7/3}$ serves as direct experimental confirmation of the r^{-6} dependence of the long-range attractive potential for K–Hg and Cs–Hg systems.

INTRODUCTION

IN a previous communication[1] preliminary measurements of rainbow scattering for the K–Hg and Cs–Hg systems were reported from which the depths of the interatomic potential wells ϵ_{12} could be evaluated. The present paper describes detailed measurements of the velocity dependence of the angular intensity distribution of K and Cs beams scattered by Hg. The low-angle behavior is of interest in that it reflects the long-range inverse sixth-power attractive part of the interatomic potential. The energy range of the rainbow scattering measurements has now been extended to achieve more precision in the determined values of the well depths, which are interpreted as the dissociation energies D_e of the $^2\Sigma^+$ ground state van der Waals molecules KHg and CsHg.

EXPERIMENTAL

The apparatus has been briefly described[2,3]; a full account of the experimental conditions of the present study is contained in the dissertation of F.A.M.[4] The main features may be briefly outlined as follows: The collimated, modulated (25 cps), primary beam of alkali is velocity selected, with a triangular velocity distribution (half-intensity width 4.7% of the nominal velocity). The alkali speed was varied over the range 185–1000 m/sec. The detector is a Pt–W ribbon surface ionizer followed by an electron multiplier, cathode follower, narrow band amplifier, phase-sensitive rectifier and recorder. The secondary (crossed) beam is a collimated thermal Hg beam; the average Hg speed was about 235 meters per second. The entire assembly of primary and secondary ovens (single-chamber Knudsen effusion type), collimating slits, beam chopper, etc., is rotated as a unit through an angle θ_a ranging from 30° in the "external quadrant" (EQ) to 60° in the "internal quadrant" (IQ) with respect to the fixed detector (in a separately pumped chamber). Typical vacua during operation were 6×10^{-7} and 2×10^{-7} Torr in the main and detector chambers, respectively. Most of the experiments were carried out in the IQ (see Appendix).

Reagents used were as follows: Hg (Mallinckrodt, reagent grade), total impurity <0.001%; K (B. and A., code 2080), analyzed to contain <1.4 atom % total impurity (principally Na); Cs (U. S. Industrial Chemical Company), analyzed to contain <1.3 atom % total impurity, principally Rb. Beams of the K and Cs have a lower level of the principal impurity due to vapor-pressure considerations.

Table I lists the important dimensions of the apparatus as employed in the present study. The symbols, s, c, d, b, u, p are, respectively, the half-widths of the source slit, collimator slit, detector, beam stop (for the detector), umbra and penumbra; l_{ij} is the distance between points i and j. Primed symbols refer to the vertical dimensions (i.e., half-heights). The effective resolution angle of the apparatus (defined according to the Kusch[5] criterion as the angle at which the efficiency

† Financial assistance from the U. S. Atomic Energy Commission, Division of Research, is acknowledged.

* H. Riggs and E. L. Macauley Fellow, Rackham Graduate School of The University of Michigan. Ph.D. dissertation, June 1962 available from University Microfilms, Ann Arbor, Michigan.

[1] F. A. Morse, R. B. Bernstein, and H. U. Hostettler, J. Chem. Phys. **36**, 1947 (1962).

[2] H. U. Hostettler and R. B. Bernstein, Rev. Sci. Instr. **31**, 872 (1960).

[3] H. U. Hostettler and R. B. Bernstein, Phys. Rev. Letters **5**, 318 (1960). These experiments involved the scattering of velocity-selected Li beams by Hg. Because of the lower reduced mass μ of this system and the deeper potential well depth ϵ_{12} (compared to the K–Hg and Cs–Hg systems), comparable values of the reduced relative kinetic energy K would have required higher Li speeds than attainable with the apparatus. Thus rainbow angles[1] for the Li–Hg system would be expected to be well outside the angular range of the experiments.

[4] F. A. Morse, Ph.D. dissertation, University of Michigan, Ann Arbor, Michigan, June 1962.

[5] P. Kusch, Notes on Angular Resolution (unpublished notes), Columbia University, New York July 1960.

TABLE I. Apparatus geometry. (All dimensions in cm).

	Primary beam	Secondary beam		Primary beam	Secondary beam
s	0.0152	0.159	s'	0.300	0.318
c	0.01905	0.159	c'	0.300	0.318
d	0.0254		d'	0.300	
b	0.0315		b'	0.300	

	Target	Detector	Target		Target	Detector	Target
u	0.0208	0.0293	0.159	u'	0.300	0.300	0.318
p	0.0317	0.111	0.273	p'	0.522	1.91	0.546
l_{bd}		1.23					
l_{sc}		10.95	1.17				
l_{cd}		29.35					
l_{ct}		4.05	0.42				
l_{td}		25.3					

Effective scattering volume = 0.0186 cm³.
Detector area = 0.031 cm².

of detection of scattering is 50%) was calculated to be 14 min of arc.

CONVERSION TO CENTER-OF-MASS SYSTEM

It is desirable to present the experimental results in terms of the differential scattering cross section $d\sigma(\theta)/d\omega$ in the center of mass (c.m.) coordinate system. The experimental data consist of measurements of the current of scattered particles (of, say, type i) into the detector of area ΔA_d subtending (at the center of the scattering zone) a solid angle $\Delta\omega_d$. The orientation of the detector is specified by the two angles θ_a, ϕ_a. These angles must be transformed to their counterpart angles θ, ϕ in the c.m. system, and the observed fluxes must be converted into differential cross sections. The resulting "experimental" $d\sigma(\theta)/d\omega$ may then be compared with theoretically calculated values to test various potential energy functions.

Although some of the following material is standard, no simple, explicit, over-all presentation has been found in the literature.[6] The present treatment is not confined to scattering in the plane defined by the incident beams and is applicable to elastic, inelastic, and/or chemically reactive scattering of crossed monochromatic beams.

We consider the idealized case of the intersection at an angle ψ of two collimated, monoenergetic beams of particles of masses m_1 and m_2; $\mathbf{v}_1$, $\mathbf{v}_2$ and $\mathbf{v}_{c.m.}$ represent the velocity vectors of particles of type 1, 2, and the c.m., respectively. Figure 1 shows the geometrical relationship between the laboratory scattering angles θ_a, ϕ_a and the c.m. angles θ, ϕ. Primed quantities designate "after the encounter." The subscript a refers to "apparatus" or laboratory quantities.

A. Deflection Angle in the c.m. vs Apparatus System

Referring to Fig. 1, the velocity vectors $\mathbf{v}_1$ and $\mathbf{v}_2$ define "the plane." The velocity vector $\mathbf{v}_1'$ of one of the scattered particles (say, type 1′) is shown directed out of the plane (for simplicity, attention is restricted to one of the scattered particles only, i.e., the type detected). Two angles specify the orientation of $\mathbf{v}_1'$: ϕ_{a1}, its elevation above the plane, and θ_{a1}, the angle from $\mathbf{v}_1$ to the projection of $\mathbf{v}_1'$ on the plane ($v_1'\cos\phi_{a1}$, as shown). The angle between $\mathbf{v}_1$ and $\mathbf{v}_{c.m.}$ is α_1. The deflection angle in the c.m. system is θ. The relative velocity is $\mathbf{v}_r=\mathbf{v}_1-\mathbf{v}_2$; its magnitude is

$$v_r=[v_1^2+v_2^2-2v_1v_2\cos\psi]^{\frac{1}{2}}. \quad (1)$$

The velocity of the incident primary beam particle relative to the c.m. is $\mathbf{w}_1$; its magnitude is

$$w_1=v_rm_2/(m_1+m_2) \quad (2)$$

(with an analogous formula for w_2). The speed of the c.m. is given by

$$v_{c.m.}=[w_1^2+v_1^2-2w_1v_1\cos\xi_1]^{\frac{1}{2}}, \quad (3)$$

where ξ_1 is the angle between $\mathbf{v}_1$ and $\mathbf{w}_1$ (as shown). The relative velocity vector $\mathbf{w}_1'$ for the scattered particle is shown rotated by the c.m. scattering angle θ with respect to the incident relative velocity $\mathbf{w}_1$.

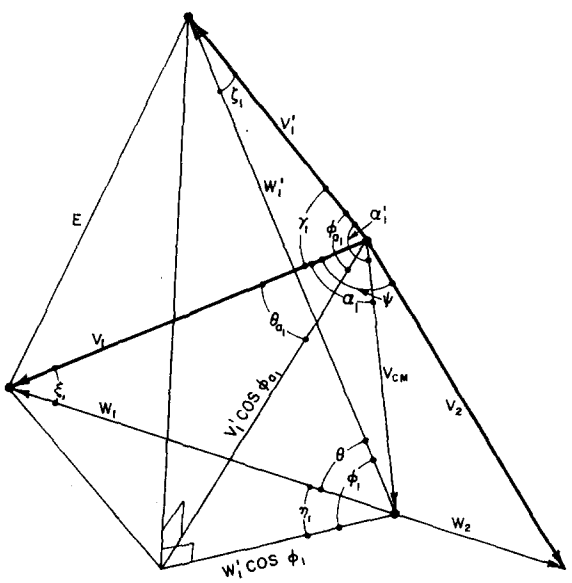

FIG. 1. Velocity diagram for the general case of scattering out of the v_1, v_2 plane. Not indicated on the drawing are vectors and angles associated with the scattered particle of type 2′.

[6] The c.m. data-conversion problem for crossed molecular beams has been considered and analyzed (in part) by several workers: (a) H. U. Hostettler and R. B. Bernstein, University of Michigan (unpublished notes), September 1958; (b) D. R. Herschbach, University of California, Rept. UCRL-9379, April 1960; (c) R. Helbing and H. Pauly, Diplomarbeit (Helbing) University of Bonn, 1961; (d) S. Datz, D. R. Herschbach, and E. H. Taylor, J. Chem. Phys. **35**, 1549 (1961); (e) E. F. Greene and J. Ross, Brown University (private communication), March 1962.

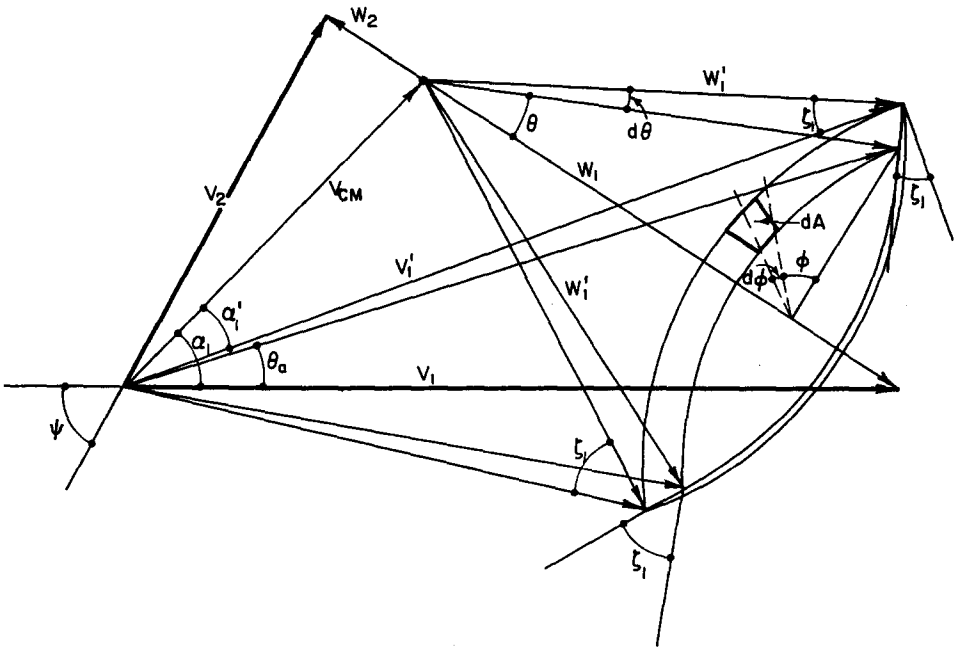

FIG. 2. Velocity diagram showing the method of evaluation of the solid angle ratio $d\omega_a/d\omega$.

The magnitude of $\mathbf{w}_1'$ is given by

$$w_1' = w_1\{(m_1m_2'/m_1'm_2)[1-(\Delta E/E_0)]\}^{\frac{1}{2}}, \quad (4)$$

with E_0 the initial relative kinetic energy ($E_0=\frac{1}{2}\mu v_r^2$) and ΔE the endothermicity, $\Delta E=\frac{1}{2}[m_1v_1^2+m_2v_2^2-m_1'v_1'^2-m_2'v_2'^2]$. For the special case of elastic scattering, of course, $w_1'=w_1$.

It is convenient to introduce the angles ϕ_1 and η_1 (analogous to ϕ_{a1} and θ_{a1}), where ϕ_1 is the angle of elevation of $\mathbf{w}_1'$ above the plane and η_1 is the angle from $\mathbf{w}_1$ to the projection of $\mathbf{w}_1'$ on the plane ($w_1'\cos\phi_1$, as shown). The angle between $\mathbf{v}_1$ and $\mathbf{v}_1'$ is γ_1. In the limit as $\phi_{a1}\to 0$, it is seen that $\phi_1\to 0$, $\gamma_1\to\theta_{a1}$ and $\eta_1\to\theta$, the standard situation for the in-plane case.

Noting that the dihedral angle between the planes containing the angles $\alpha_1-\theta_{a1}$ and ϕ_{a1} is $\pi/2$, such that $\cos\alpha_1'=\cos(\alpha_1-\theta_{a1})\cos\phi_{a1}$, one evaluates the magnitude of v_1':

$$v_1' = v_{\text{c.m.}}\cos\alpha_1' \pm [v_{\text{c.m.}}^2\cos^2\alpha_1' - v_{\text{c.m.}}^2 + w_1'^2]^{\frac{1}{2}}. \quad (5)$$

Next, one relates θ_{a1} to θ by utilizing the common length E:

$$w_1'^2+w_1^2-2w_1'w_1\cos\theta = E^2 = v_1'^2+v_1^2-2v_1'v_1\cos\gamma_1, \quad (6)$$

with $\cos\gamma_1=\cos\theta_{a1}\cos\phi_{a1}$. Finally, rearrangement of Eq. (6) yields

$$\theta = \arccos\left[\frac{w_1^2+w_1'^2-(v_1^2+v_1'^2)+2v_1v_1'\cos\theta_{a1}\cos\phi_{a1}}{2w_1w_1'}\right]. \quad (7)$$

Thus, given the laboratory scattering angles θ_{a1} and ϕ_{a1}, one may calculate the corresponding c.m. scattering angle θ.

For the special cases of in-plane elastic scattering, $\phi_{a1}=\phi_1=0$, $w_1'=w_1$, and Eq. (7) reduces to

$$\theta = \arccos[(2w_1^2-v_1^2-v_1'^2+2v_1v_1'\cos\theta_{a1})/2w_1^2]. \quad (8)$$

In addition, $\alpha_1'=\alpha_1-\theta_{a1}$ and

$$\alpha_1 = \arccos[(v_{\text{c.m.}}^2+v_1^2-w_1^2)/2v_1v_{\text{c.m.}}] \quad (9)$$

For the common case of $\psi=90°$ (right-angle crossed beams), Eq. (3) simplifies to

$$v_{\text{c.m.}} = (w_1^2+v_1^2-2w_1v_1^2/v_r)^{\frac{1}{2}} = (m_1^2v_1^2+m_2^2v_2^2)^{\frac{1}{2}}/(m_1+m_2); \quad (10)$$

here $v_r=(v_1^2+v_2^2)^{\frac{1}{2}}$; w_1 is given by Eq. (2) as before.

B. Differential Cross Section in the c.m. versus Apparatus System

Returning now to the general case, the intensity (number per unit time per unit of solid angle) of scattered particles of the specified type i measured at the detector located at θ_a, ϕ_a is

$$I_i(\theta_a,\phi_a) = \frac{\Delta F_i(\theta_a,\phi_a)}{\Delta\omega_d} = n_1n_2v_r\Delta V\frac{d\sigma_i(\theta_a,\phi_a)}{d\omega_a}, \quad (11)$$

where ΔF_i is the flux or current (number per unit time) received by the detector, n_1 and n_2 are the number densities of the colliding particles (types 1 and 2, respectively), ΔV the volume of the collision zone, and $d\sigma_i(\theta_a,\phi_a)/d\omega_a$ the differential scattering cross section in the apparatus system. The differential cross section in the c.m. system is

$$\frac{d\sigma_i(\theta)}{d\omega} = \frac{d\sigma_i(\theta_a,\phi_a)}{d\omega_a}\frac{d\omega_a}{d\omega}. \quad (12)$$

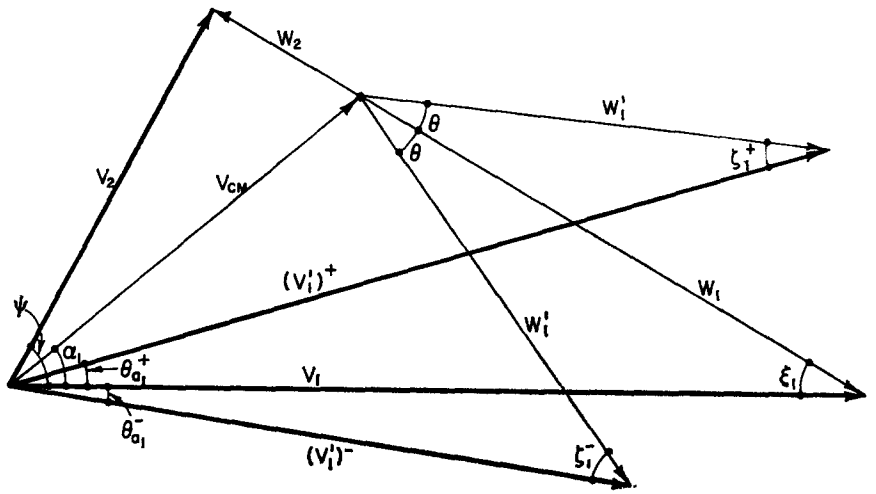

FIG. 3. Projection on the v_1, v_2 plane of Fig. 2, illustrating the special case of in-plane scattering. Positive signs denote the IQ, negative signs the EQ.

Figure 2 allows evaluation of the solid angle ratio $d\omega_a/d\omega$, confining attention to the scattered particles of one specified type, say, type 1′. It is seen that an element of area on the c.m. ring, dA, subtends a solid angle at the c.m. of $d\omega=dA/w_1'^2$, while subtending a solid angle at the center of the scattering zone of $d\omega_a=dA\mid\cos\zeta_1\mid/v_1'^2$.
Thus

$$d\omega_a/d\omega=(w_1'/v_1')^2\mid\cos\zeta_1\mid. \tag{13}$$

It is noted that ζ_1 and v_1' are functions of ϕ.

Combining Eqs. (11), (12), and (13) we have, explicitly,

$$\frac{d\sigma(\theta)}{d\omega}=\frac{I_1(\theta_a,\phi_a)}{n_1n_2v_r\Delta V}\left(\frac{w_1'}{v_1'}\right)^2\mid\cos\zeta_1\mid, \tag{14}$$

where

$$\cos\zeta_1=(w_1'^2+v_1'^2-v_{\text{c.m.}}^2)/2w_1'v_1'. \tag{15}$$

Although $d\sigma(\theta)/d\omega$ is independent of ϕ, the observable scattering $I_1(\theta_a,\phi_a)$ is not axially symmetric.

Figure 3 shows a projection, on the plane, of a velocity diagram such as Fig. 2 to illustrate the special case of in-plane scattering. Here we see two laboratory angles $(\theta_{a1})^+$ and $(\theta_{a1})^-$, located respectively in the IQ and EQ regions, corresponding to the same c.m. scattering angle θ. It is seen that the observable intensity of scattering will be different for the detector at (θ_{a1}^+) and $(\theta_{a1}^-,0)$; the ratio is [from Eq. (14)]:

$$\frac{I_1(\theta_{a1}^-,0)}{I_1(\theta_{a1}^+,0)}=\left[\frac{(v_1')^-}{(v_1')^+}\right]^2\frac{\mid\cos\zeta_1^+\mid}{\mid\cos\zeta_1^-\mid}\neq 1. \tag{16}$$

In the Appendix experimental results on the asymmetry of scattering in the apparatus system (IQ vs EQ) are presented, which illustrate the applicability of Eqs. (14) and (16). In the limit as $\alpha_1\to 0$, one notes that $(v_1')^-/(v_1')^+\to 1$, $\zeta_1^+/\zeta_1^-\to 1$, and $\theta_{a1}^+/\theta_{a1}^-\to 1$, i.e., axial symmetry obtains.

To obtain $d\sigma(\theta)/d\omega$ from Eq. (14) in the practical case, where the primary beam is not negligibly attenuated by scattering, n_1 must be replaced by a suitable average.[7] For a scattering zone of finite length, the volume of the scattering (target) zone is $\Delta V=A_t l$, where l is the length of the zone (traversed by the primary beam) and A_t is the cross-sectional area of that beam through the target zone.

The average value of n_1 is

$$\bar{n}_1=l^{-1}\int_0^l n_1(x)\,dx=\frac{n_1(0)\,(1-T_1)}{\ln(1/T_1)}, \tag{17}$$

while $\bar{n}_2$ is

$$\bar{n}_2\cong\frac{v_1}{v_r}\frac{\ln(1/T_1)}{\sigma(\theta_0)l}, \tag{18}$$

where $\sigma(\theta_0)$ is the "total" cross section for scattering into laboratory angles greater than θ_0, the "resolution angle"; T_1 is the primary beam transmission [i.e., $T_1=1-\Delta S_1(0,0)/S_1(0,0)$], where $S_1(0,0)$ is the observed primary beam signal at the detector and $\Delta S_1(0,0)$ is the loss in signal due to the scattering. Here $n_1(0)$ is the number density of particles in the primary beam incident to the scattering zone and $n_1(0)=F_1(0,0)/v_1A_t$, where $F_1(0,0)$ is the total current of primary beam which would reach the detector plane in the absence of scattering. Since the size of the detector is less than the cross-sectional area of the (diverging) beam at the detector plane, the measured primary beam signal is smaller than this total current by a (known) geometrical factor G, i.e., $S_1=F_1/G$. Appropriate substitution into Eq. (14) yields

$$\frac{d\sigma(\theta)}{d\omega}=I_1(\theta_a,\phi_a)\left(\frac{w_1'}{v_1'}\right)^2\mid\cos\zeta_1\mid\frac{v_1}{v_r}\frac{\ln(1/T_1)}{(1-T_1)\bar{n}_2lGS_1(0,0)}. \tag{19}$$

[7] The averaging of n_2 is not a serious problem since it may be regarded as constant; for most crossed beam experiments the secondary beam path length across the primary beam is usually very short and its transmission through the scattering zone is nearly 100%.

Unfortunately, it is often difficult to obtain an accurate measure of $\bar{n}_2$. To obviate the need for its evaluation, Eq. (19) may be transformed to give a ratio of differential to "total" cross sections which is adequate for most purposes. Equation (18) relates $\bar{n}_2$ to $\sigma(\theta_0)$; the velocity dependence of $\sigma(\theta_0)$ may be written $\sigma(\theta_0)=\sigma_0 v_r^{-j}$, where j may be determined experimentally for a given apparatus resolution. For

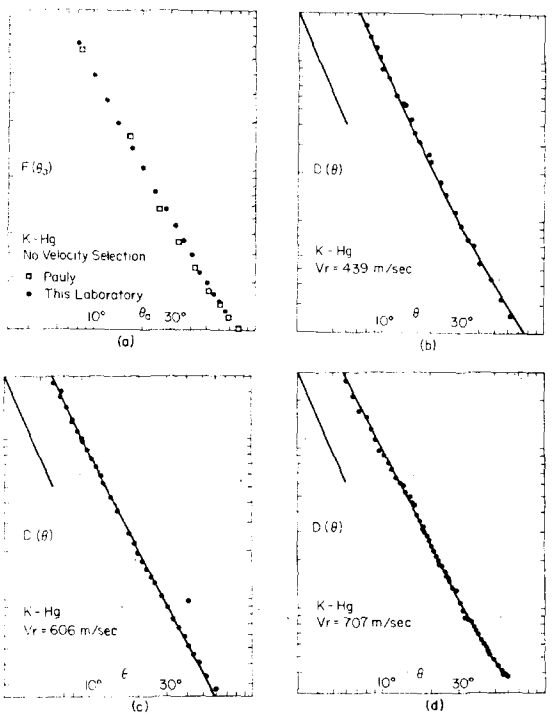

FIG. 4. (a) Comparison of the observed angular distribution for the scattering of thermal K by a crossed thermal Hg beam: □ Data of Pauly.[10] ● Present results. (b), (c), and (d) $D(\theta)$ for K–Hg at specified values of $\bar{v}_r$. Throughout, angles are in degrees. Note that in each figure [4(b)–7] the solid curve represents the best fit to the data from several [i.e., 2–8] replicate experiments, while the points are for a single run.

θ_0 sufficiently small, $j=\frac{2}{5}$, the Massey–Mohr[8] velocity dependence. Substitution leads to

$$\frac{d\sigma(\theta)}{d\omega}\Big/\sigma_0=\frac{F_1(\theta_a,\phi_a)}{\Delta S_1(0,0)}v_r^{-2/5}\left(\frac{w_1'}{v_1'}\right)^2|\cos\zeta_1|\frac{l_{td}^2}{GA_d}. \tag{20}$$

Thus one may define a relative differential cross section $D(\theta)$, from which the velocity dependence of the total cross section has been removed:

$$D(\theta)\equiv\left[\frac{d\sigma(\theta)}{d\omega}\Big/\sigma_0\right]\frac{GA_d}{l_{td}^2}=\frac{F_1(\theta_a,\phi_a)}{\Delta S_1(0,0)}v_r^{-2/5}\left(\frac{w_1'}{v_1'}\right)^2|\cos\zeta_1|. \tag{21}$$

The behavior of $D(\theta)$ as a function of v_r may be directly compared with that of $d\sigma(\theta)/d\omega$ calculated theoretically.

[8] H. S. W. Massey and C. B. O. Mohr, Proc. Roy. Soc. (London) **A144**, 188 (1934).

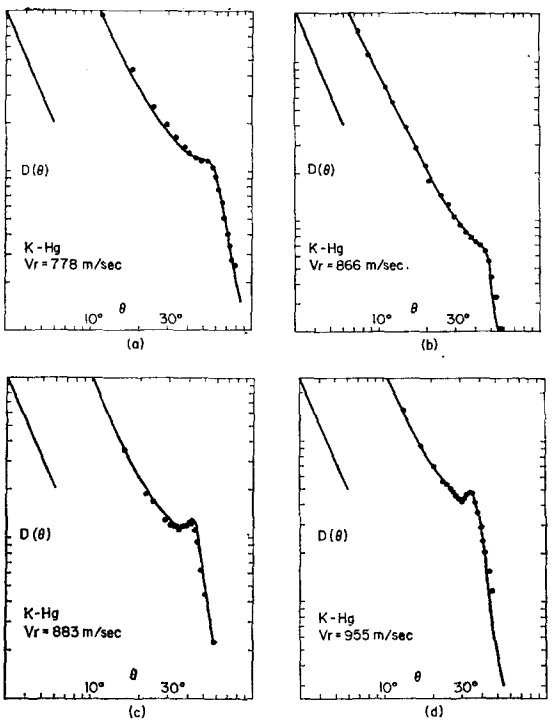

FIG. 5. $D(\theta)$ for K–Hg at specified values of $\bar{v}_r$.

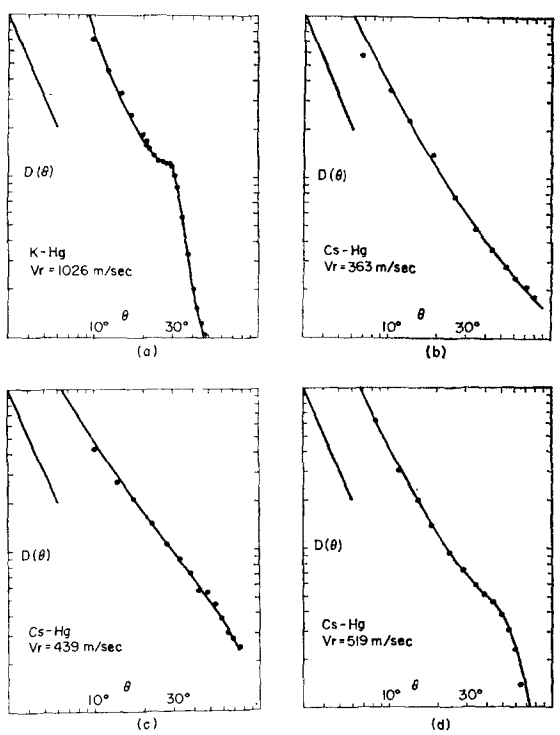

FIG. 6. $D(\theta)$ for K–Hg at specified $\bar{v}_r$. (b), (c), and (d) $D(\theta)$ for Cs–Hg at specified values of $\bar{v}_r$.

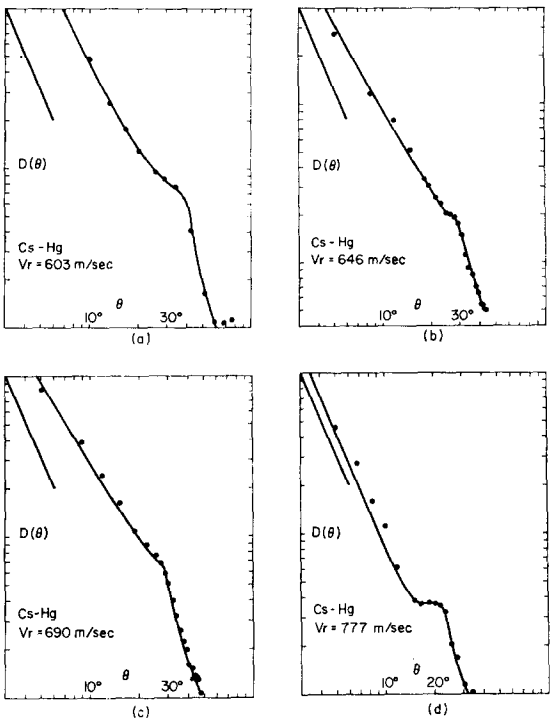

FIG. 7. $D(\theta)$ for Cs–Hg at specified values of $\bar{v}_r$.

RESULTS AND DISCUSSION

A. Comparison with Literature

Pauly has reported[9] the angular distribution of the scattering of a thermal K beam by a crossed beam of Hg (both beams with a Maxwellian velocity distribution). As a preliminary to the present study with velocity-selected alkali beams, a comparison with Pauly's[10] experimental results was desirable; thus the angular intensity distribution of scattering for a thermal K beam (without velocity selection) was carried out under conditions[11] comparable to his. The results are shown in Fig. 4(a), using a log–log representation. The two sets of data are expressed in arbitrary intensity units adjusted to coincide at a laboratory scattering angle $\theta_a = 60°$. Agreement is satisfactory.

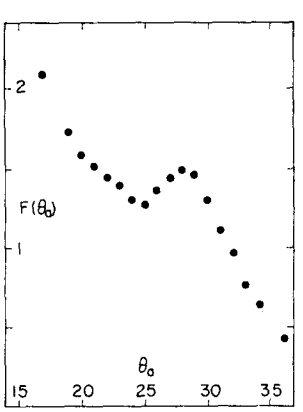

FIG. 8. Observed data [linear coordinate plot of $F(\theta)_a$] showing the detail of a well-resolved rainbow maximum. K–Hg; $v_1 = 927$, $\bar{v}_2 = 230$, $\bar{v}_r = 955$ m/sec.

[9] H. Pauly, Z. Naturforsch. **14A**, 1083 (1959).
[10] H. Pauly, University of Bonn (private communication), March 1961.
[11] $T_K = 450°K$, $T_{Hg} = 365°K$.

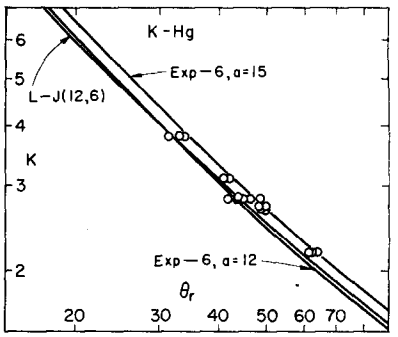

FIG. 9. Energy dependence of θ_r for K–Hg. The solid lines are calculated from the indicated potentials. The points are the experimental data using $\epsilon = 7.4_6 \times 10^{-14}$ erg.

B. New Experimental Results

The velocity dependence of $D(\theta)$ is shown in Figs. 4–7. Log-log plots are used. In each figure the *solid curve* represents the best fit to the data from *several* [i.e., 2–8] replicate experiments, while the *points* shown are for *one* representative run. The straight line segment at the upper left corner of each plot is drawn with the classical theoretical[12] limiting low-angle slope of $-\frac{7}{3}$ for comparison with the data. The agreement serves as direct experimental confirmation[13] of an inverse-sixth-power long-range attractive potential for the systems K–Hg and Cs–Hg.

Figure 8 shows the detail of an experimentally well-

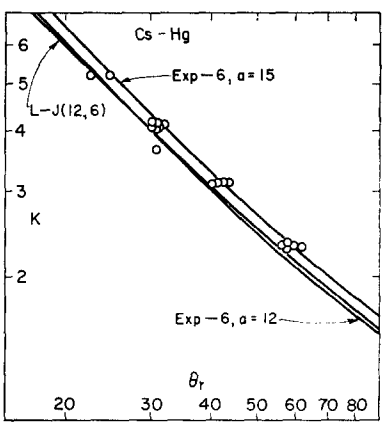

FIG. 10. Energy dependence of θ_r for Cs–Hg. The solid lines are calculated from the indicated potentials. The points are the experimental data using $\epsilon = 7.7_2 \times 10^{-14}$ erg.

[12] See, for example, E. H. Kennard, *Kinetic Theory of Gases* (McGraw-Hill Book Company, Inc., New York, 1938), p. 120. Assume $V(r) = -C/r^6$ and small θ (i.e., $\sin\theta \cong \theta$).
[13] R. Helbing and H. Pauly [Z. Physik (to be published); also reference 6(c)] have obtained similar evidence for the systems K–Ar, –Xe, –Br_2, etc., from measurements of the low-angle scattering of thermal K beams (no velocity selection).

TABLE II. Potential well depths (present experiments).

System	ϵ_{12}(erg)	ϵ/k(°K)
K–Hg	$7.4_8\times10^{-14}$	539
Cs–Hg	$7.7_2\times10^{-14}$	558

resolved rainbow maximum. Plotted (using linear scales) is the directly observed intensity of scattering as a function of laboratory angle, i.e., $F(\theta_a)$.

Figures 9 and 10 show the energy dependence of θ_r, the rainbow angle [defined[1] as the outer inflection point after the "hump," obtained from (linear coordinate) plots of $D(\theta)$]. The procedure of reference 1 was employed to analyze the data. That is, plots of $\log E_0$ vs $\log\theta_r$ were vertically adjusted (i.e., at constant θ_r) to give the best fit to the band of theoretical $\log K$ vs $\log\theta_r$ lines (as usual $K=E_0/\epsilon_{12}$, the reduced relative kinetic energy). A number of additional data points were available so that the derived potential well depths (Table II) are more reliable than the earlier[1] values. The estimated precision in the ϵ_{12} determination is $\pm5\%$. The major uncertainty involves the question of the sensitivity of the theoretical $K(\theta_r)$ function to the "shape" of the potential.

The present results for ϵ_{12} are not inconsistent with (necessarily rough) semiempirical estimates, made as follows. Individual ϵ_i values were approximated taking cognizance of viscosity data for Hg and making use of relations[14] obtained via the corresponding-states principle involving the melting points (alternatively, the boiling points) of K and Cs. The usual combining rule $\epsilon_{12}=(\epsilon_1\epsilon_2)^{\frac{1}{2}}$ was employed. The values of ϵ_{12}/k thus

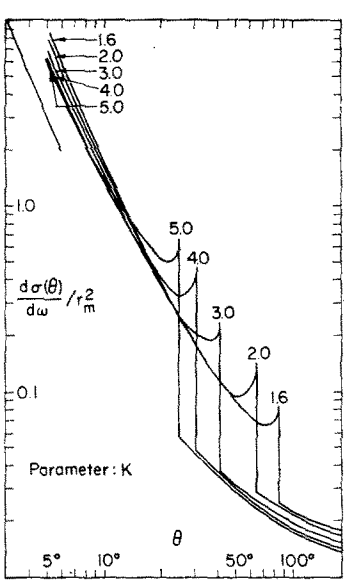

FIG. 11. Reduced differential cross sections as a function of K for the exp-6 ($\alpha=12$) potential (from Mason's tables[15]).

[14] See, for example, procedures in J. O. Hirschfelder, C. F. Curtiss, and R. B. Bird, *Molecular Theory of Gases and Liquids* (John Wiley & Sons, Inc., New York, 1954).

TABLE III. Summary of observed $D(17°)$ values.

K–Hg		Cs–Hg	
v_r(m/sec)	$10^6\times D(17°)$	v_r(m/sec)	$10^6\times D(17°)$
1026	2.2	777	3.7
955	1.0	690	1.2
883	3.1	646	3.7
866	2.8	603	1.7
778	4.5	519	1.7
707	3.5	439	2.1
606	2.7	363	1.5
439	3.1		

obtained ranged from 540°–920°K for K–Hg and 510°–890°K for Cs–Hg.

Assuming an exp-6 potential, Mason[15] has calculated "reduced" classical[16] differential cross sections as a function of K. Figure 11 shows a plot of $d\sigma^*(\theta)/d\omega\equiv r_m^{-2}[d\sigma(\theta)/d\omega]$ for relevant K's, assuming one value of the repulsive index, $\alpha=12$. These curves are seen to converge near $\theta=17°$. For comparison, experimental average values of $D(\theta)$ at 17° are collected in Table III. The results are disappointing; the discrepancies are greater than anticipated, even after taking into consideration the fact that accurate measurements of the transmission had not been made with each run. The only conclusion that may fairly be drawn from Table III is that there is no significant trend of $D(17°)$ with relative velocity, in accord with expectation.

For the purpose of obtaining absolute values of $d\sigma(\theta)/d\omega$ from $D(\theta)$, one combines Eqs. (19) and (21) to obtain

$$d\sigma(\theta)/d\omega=D(\theta)\,(l_{id}^2/GA_d l\bar{n}_2)\,v_1 v_r^{-3/5}\ln(1/T_1). \quad (22)$$

Then, by fitting an experimental $d\sigma(\theta)/d\omega$ curve to the

TABLE IV. Estimated r_m values.

Method	System	r_m(Å)	Ratio: CsHg/KHg
1. From exptl ϵ_{12} and SK formula	Cs–Hg	4.13	1.03
	K–Hg	4.00	
2. Metallic radii	Cs–Hg	4.14	1.08
	K–Hg	3.83	
3. Molar volume	Cs–Hg	4.49	1.09
	K–Hg	4.11	

[15] E. A. Mason, J. Chem. Phys. **26**, 667 (1957).

[16] K. W. Ford and J. A. Wheeler [Ann. Phys. (N. Y.) **7**, 287 (1959)] have shown that the classical rainbow infinity (cusp) becomes a smooth maximum according to the semiclassical analysis.

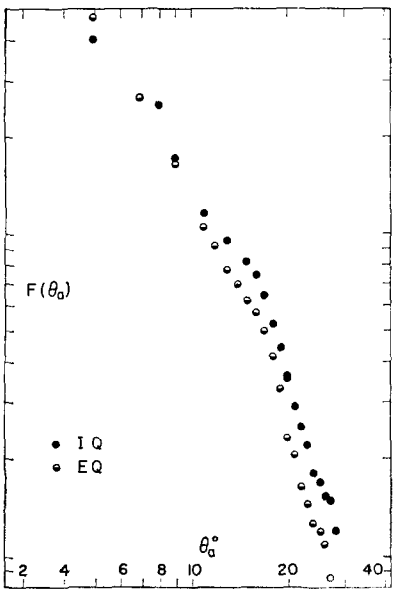

FIG. 12. Asymmetry of scattering as observed in the apparatus system.

calculated curve of $d\sigma^*(\theta)/d\omega$, r_m may be found:

$$r_m=\left[\frac{d\sigma(\theta)}{d\omega}\Big/\frac{d\sigma^*(\theta)}{d\omega}\right]^{\frac{1}{6}}. \tag{23}$$

Unfortunately, the present experiments have not yielded accurate absolute values of $d\sigma(\theta)/d\omega$. This is the case not only because of the aforementioned lack of precision of $D(\theta)$, but also because of a possible systematic error in connection with evaluating $\bar{n}_2$. Since $\bar{n}_2$ calculated on the basis of ideal effusion from the secondary oven will always be higher[17] than the true value (by a factor estimated to lie in the range 1–10), calculated cross sections will be low and the derived r_m values [Eq. (23)] will represent only lower limits. Nevertheless, the calculations were carried out for a number of representative experiments, yielding for lower limits of r_m the values 2.1 Å for Cs–Hg and 1.7$_5$ Å for K–Hg. The ratio of these is, of course, more reliable than the individual values (since the systematic error in $\bar{n}_2$ will tend to cancel out). Thus one obtains r_m(Cs–Hg)/r_m(K–Hg)$\cong$1.2.

An alternative procedure for extracting r_m values from the data is to make use of calculated dispersion energies; the long-range attractive potential constant is given by $C=2\epsilon r_m^6$ (for $\alpha=12$). The Slater–Kirkwood (SK) formula for C (applied previously[18] in connection with estimating total cross sections for scattering of K and Cs by scattering a number of different gases) was used. If one assumes polarizabilities (Å^3) as follows: Hg, 5.1[19]; Cs, 52.5[20]; K, 36.0[20]; calculated dispersion constants C (in units of 10^{-60} erg cm^6) of 762 and 608 for Cs–Hg and K–Hg, respectively, are obtained. Then, using the present values for ϵ_{12} (Table II) one obtains r_m values, listed in Table IV. For comparison, Table IV also includes estimates of r_m based on considerations of metallic radii and molar volumes.[14]

A more precise "experimental" determination of r_m by the C procedure would require absolute measurements of the total scattering cross section, from which an "experimental" C could be obtained. Then, using ϵ_{12} evaluated from the rainbow angle a more reliable value of r_m could be calculated. To achieve an uncertainty of, say, $\pm 3\%$ in r_m by this method an accuracy of better than 20% in the C/ϵ ratio would be required.

One final comment appears desirable. Care must be taken to ensure proper interpretation of scattering data designed to yield information about potential energy functions. In general (even in the case of the scattering of pairs of ground state atoms), more than one potential curve, i.e., several molecular states, may be involved. For example, $K(^2S_{\frac{1}{2}})+Hg(^1S_0)\rightarrow KHg(^2\Sigma^+)$ but $K(^2S_{\frac{1}{2}})+Cs(^2S_{\frac{1}{2}})\rightarrow KCs(^1\Sigma^+)$ *and* $KCs(^3\Sigma^+)$. Therefore, measured K–Cs scattering cross sections would be

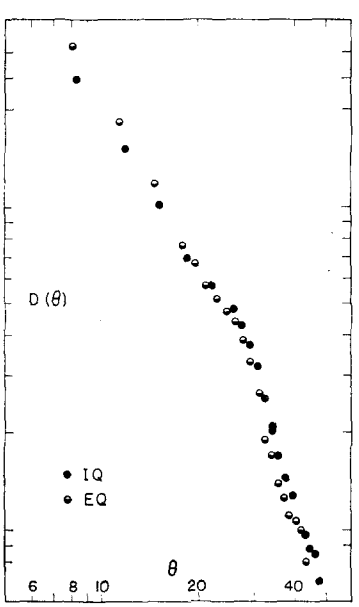

FIG. 13. Symmetry of scattering after conversion of results to the c.m. system.

[17] One of the major difficulties in evaluating $\bar{n}_2$ is the question of "cloud formation" in front of the secondary oven slit, and the attendant scattering which produces a serious alteration of the velocity distribution and an appreciably lower net intensity of the secondary beam at the target zone. For $T_{Hg}=365$°K, $P_{Hg}=0.16$ mm Hg; *cf.* $T_K=450$°K, $P_K=2.5\times10^{-3}$ mm Hg.

[18] E. W. Rothe and R. B. Bernstein, J. Chem. Phys. **31**, 1619 (1959).

[19] From Landolt-Börnstein, *Physikalisch-Chemische Tabellen* (Springer-Verlag, Berlin, 1950) 6th ed., I. Band, 3. Teil, with α calculated from molar polarization on p. 514; a corresponding value is listed in I. Band, 1. Teil, p. 401. Since the calculated C depends nearly linearly upon α (Hg) and also upon α (K or Cs), the uncertainty in α values lead to serious errors. In addition, the SK formula is only approximate; thus the C values quoted must be regarded as semiquantitative estimates. Ratios of C's are, of course, more reliable due to cancellations.

[20] A. Salop, E. Pollack, and B. Bederson, Phys. Rev. **124**, 1431 (1961).

a 1:3 weighted average of (quite different) singlet and triplet cross sections. Only in the case of scattering by ^1S atoms will the cross sections yield information unequivocally about a single molecular state.

ACKNOWLEDGMENT

The authors appreciate the valuable contributions to this work made by Dr. H. U. Hostettler, who was primarily responsible for the design and construction of the apparatus and who participated in many useful discussions.

APPENDIX

Asymmetry of Scattering in the Apparatus System

As a test of possible systematic apparatus bias, certain check runs were carried out in which angular distributions of scattering were measured in both quadrants (IQ and EQ). The data for one such experiment (Cs–Hg, $v_1=649$, $\bar{v}_2=234$, $\bar{v}_r=690$ m/sec) are presented in Fig. 12. As anticipated [cf. Eq. (16)] the observed distributions $F(\theta_a)$ are not symmetrical. However, conversion of the data to the c.m. system led to the expected symmetry in $D(\theta)$, as shown in Fig. 13 (the deviations at low angles are associated with the great steepness of the angular distribution in this region and the experimental difficulty in reproducing the low-angle settings).

The conversion of data from the IQ to the c.m. was found to be less sensitive (than the conversion of comparable EQ data) to the somewhat arbitrary choice of "average" or "effective" velocity of the secondary beam, $\bar{v}_2$. This is seen in Fig. 3. Upon making a small change of v_2 and thus $v_{c.m.}$ the values of v_1', ζ_1, and θ_{a1} in the IQ are relatively unaffected, but the same quantities (particularly θ_{a1}) in the EQ change significantly. This led to the adoption of the IQ as the "standard" quadrant for the main body of the measurements.

THE JOURNAL OF CHEMICAL PHYSICS VOLUME 37, NUMBER 9 NOVEMBER 1, 1992

Benzene Ring Distortion by One Substituent. Microwave Determination of the Complete Structure of Benzonitrile

BØRGE BAK, DANIEL CHRISTENSEN, WILLIAM B. DIXON,* LISE HANSEN-NYGAARD, AND JOHN RASTRUP-ANDERSEN
Chemistry Department, University of Copenhagen, Copenhagen, Denmark

(Received July 13, 1962)

Microwave spectra of benzonitrile, C_6H_5CN, and 9 isotopic species are reported. Moments of inertia of these 10 molecules are combined to give the r_s structure of benzonitrile. The final structure is: C(1)C(2) = 1.391 Å, C(2)C(3) = 1.393 Å, C(3)C(4) = 1.400 Å, C(1)C(7) = 1.455 Å, C≡N = 1.159 Å, C(2)H(2) = 1.069 Å, C(3)H(3) = 1.082 Å, C(4)H(4) = 1.081 Å, C(6)C(1)C(2) = 122.5°, C(1)C(2)C(3) = 118.45°, C(2)C(3)C(4) = 120.3°, C(3)C(4)C(5) = 120.0°, C(1)C(2)H(2) = 121.8°, C(4)C(3)H(3) = 119.9°.

INTRODUCTION

IN order to get insight into the magnitude of the geometrical changes of the benzene gas molecule, occurring by substitution of one of its hydrogen atoms, microwave spectra of nine isotopic species of benzonitrile, C_6H_5CN (I), were investigated. As far as known to us this experimental method, although by no means ideal, is the only one available to treat this type of problem.

The nine isotopic species are the three *mono*-deuterated species; the four *mono*-^{13}C(ring) species, and the species $C_6H_5\,^{13}CN$ and $C_6H_5C^{15}N$. All the samples were enriched, the deuterated samples to 100%, the remaining samples to various concentrations between 10 and 55%.[1–3]

The substituent, the CN group, was chosen because its alleged mesomeric and inductive effects work in the same direction, both provoking electrons to withdraw from the benzene ring. This helps in making the investigation conclusive. The geometrical changes found are small, but they cannot be interpreted as resulting from cancellation of mesomeric and inductive effects.

The CN group is known to exert about average substituent effects in the benzene ring. In the first place, the mesomeric dipole moment, taken as the difference between the dipole moment of (I), 4.14 D, and the dipole moment of tertiary butyl cyanide, $(CH_3)_3CCN$ (II), 3.95 D, is of medium magnitude, ~0.20D. Secondly, the chemical shifts of the protons of (I) relative to the benzene protons is of normal magnitude, ~20 cps at 14 900 Oe (gauss). As a third point of importance (although perhaps quite indirect), the CN group belongs to the meta-directing substituents. On nitration of (I), the quantity of meta derivative is about eight times the combined quantities

* Present address: National Research Council, Ottawa, Canada.

[1] B. Bak and J. T. Nielsen, Z. Elektrochem. **64**, 560 (1960).

[2] B. Bak, J. T. Nielsen, and L. Lipschitz, Acta Chem. Scand. **15**, 949 (1961).

[3] B. Bak, J. J. Christiansen, L. Lipschitz, and J. T. Nielsen, Acta Chem. Scand. (to be published).